

LOW INTENSITY VIBRATIONS RESTORE NUCLEAR YAP LEVELS AND ACUTE
YAP NUCLEAR SHUTTLING IN MESENCHYMAL STEM CELLS SUBJECTED TO
SIMULATED MICROGRAVITY

by

Matt Thompson



A thesis

submitted in partial fulfillment

of the requirements for the degree of

Master of Science in Mechanical Engineering

Boise State University

May 2020

© 2020

Matt Thompson

ALL RIGHTS RESERVED

BOISE STATE UNIVERSITY GRADUATE COLLEGE

DEFENSE COMMITTEE AND FINAL READING APPROVALS

of the thesis submitted by

Matt Thompson

Thesis Title: Low Intensity Vibrations Restore Nuclear YAP Levels and Acute YAP Nuclear Shuttling in Mesenchymal Stem Cells Subjected to Simulated Microgravity

Date of Final Oral Examination: 14 April 2020

The following individuals read and discussed the thesis submitted by student Matt Thompson, and they evaluated his presentation and response to questions during the final oral examination. They found that the student passed the final oral examination.

Gunes Uzer, Ph.D. Chair, Supervisory Committee

Clare Fitzpatrick, Ph.D. Member, Supervisory Committee

Xinzhu Pu, Ph.D. Member, Supervisory Committee

The final reading approval of the thesis was granted by Gunes Uzer, Ph.D., Chair of the Supervisory Committee. The thesis was approved by the Graduate College.

DEDICATION

I would like dedicate this thesis to my father John Thompson and to my mother Lisa Thompson, for their unrelenting support of my studies and career building and for the work ethic which they demonstrated and passed on to me, without all of which I would not have accomplished this significant work.

ACKNOWLEDGEMENTS

The completion of this work necessitates that I acknowledge several individuals who contributed significantly to its success. First and foremost, the invaluable advice and feedback provided by Dr. Gunes Uzer for the research in this study was instrumental in its execution and exemplary for his role as my major advisor. Additionally, the support and commentary from my thesis committee members Dr. Clare Fitzpatrick and Dr. Xinzhu Pu contributed substantially to the quality of this document and the presentation of this research. Finally, sections of the methods utilized in this research were developed through diligent work by other research students including the image analysis MATLAB code process assembled by Kali Woods and the atomic force microscopy procedure developed by Josh Newberg. These were both crucial contributing components of this research which enabled me to accomplish the experiments described in this document.

ABSTRACT

The bone deterioration that astronauts experience in microgravity environments is known to occur in response to the lack of gravity-based tissue stress. Mechanical forces are crucial to maintain healthy bone mass by regulating the function of bone-making osteoblasts as well as the proliferation and differentiation of their progenitors, mesenchymal stem cells (MSC) which replenish osteoblastic cells. Regulation of proliferative function of MSCs in response to mechanical force is in part controlled by the “mechanotransducer” protein YAP (Yes-associated protein) which is shuttled into the nucleus in response to mechanical challenge to induce gene expression necessary for cell proliferation. Our group had recently reported that altered gravity conditions under simulated microgravity (SMG) decreases proliferation of MSCs and that application of daily low intensity vibrations (LIV) during SMG reverses this effect on proliferation. While these findings suggest that LIV may be a promising countermeasure for altered loading, the specific SMG and LIV effects on YAP mechanosignaling are unknown. Therefore, here we tested the effects of SMG and daily LIV treatment on basal nuclear YAP levels as well as on the acute YAP nuclear entry in response to both mechanical and soluble factors in MSCs. MSCs subjected to 72h of SMG, despite decreased nuclear YAP levels across all groups, responded to both LIV and Lysophosphohaditic acid (LPA) treatments by increasing nuclear YAP levels within 6hrs by 49.52% and 87.34%, respectively. Additionally, daily LIV restored the basal decrease seen in SMG as well as nuclear YAP levels as well as restored in part the YAP nuclear entry response to

subsequently applied acute LIV and LPA treatments. These results show that rescue of basal YAP levels by LIV may explain previously found proliferative effects of MSCs under SMG and demonstrates that daily LIV is capable of alleviating the inhibition caused by SMG of YAP nuclear shuttling in response to subsequent mechanical and soluble challenge.

TABLE OF CONTENTS

DEDICATION	iv
ACKNOWLEDGEMENTS	v
ABSTRACT	vi
LIST OF FIGURES	xi
LIST OF ABBREVIATIONS	xii
CHAPTER ONE: INTRODUCTION.....	1
1.1 Research Motivation:	1
1.2 Specific Experimental Goal	1
CHAPTER TWO: BACKGROUND	3
2.1 Tissue Forces	3
2.1.1 Microgravity	3
2.1.2 Low Intensity Vibrations	3
2.2 Mechanoadaptive Regeneration	5
2.2.1 Cell Mechanoadaptation	5
2.2.1 Mesenchymal Stem Cells.....	5
2.3 Mechanoadaptive Signaling.....	7
2.3.1 Cell Signaling Pathways	7
2.3.2 YAP Signaling Pathway	8
CHAPTER THREE: DEVELOPMENT OF METHODS.....	9

3.1 Mechanical Treatments.....	9
3.1.1 Low Intensity Vibrations Treatment.....	9
3.1.2 Simulated Microgravity Treatments	10
3.2 Protein Tracking using Immunofluorescence Microscopy.....	11
3.2.1 YAP Immunofluorescence Staining	11
3.2.2 Stained Sample Imaging	12
3.2.3 Image Analysis.....	12
CHAPTER FOUR: MANUSCRIPT. “LOW INTENSITY VIBRATIONS RESTORE NUCLEAR YAP LEVELS AND ACUTE YAP NUCLEAR SHUTTLING IN MESENCHYMAL STEM CELLS SUBJECTED TO SIMULATED MICROGRAVITY”	14
4.1 Abstract.....	15
4.2 Introduction.....	16
4.3 Results.....	19
4.3.1 Acute LIV Application Increases Nuclear YAP Levels	19
4.3.2 Basal Nuclear YAP Levels Decreased by SMG Were Rescued by LIV	20
4.3.3 LIV _{AT} -induced YAP Nuclear Entry Decreased by SMG Was Partially Restored by Daily LIV _{DT} Application.....	21
4.3.4 LPA Addition Increases Nuclear YAP Levels.....	24
4.3.5 LPA-induced YAP Nuclear Entry Decreased by SMG Was Partially Restored by Daily LIV _{DT} Application	25
4.3.6 SMG and LIV _{DT} Do Not Affect Nuclear Stiffness or Nuclear Area	27
4.4 Discussion.....	28
4.5 Methods.....	32
4.5.1 Mesenchymal Stem Cell Culture	32

4.5.2 Low Intensity Vibrations Treatment	32
4.5.3 Simulated Microgravity Treatment	33
4.5.4 Immunofluorescence Staining and Image Analysis.....	33
4.5.3 Atomic Force Microscopy	34
4.5.3 Simulated Microgravity Treatment	34
CHAPTER FIVE: RESEARCH CONCLUSIONS AND FUTURE	36
5.1 Summary of Research.....	36
5.2 Current Limitations	37
5.3 Future Directions	37
REFERENCES	39

LIST OF FIGURES

Figure 1.	Application of low intensity vibrations (a) in vivo (b) in vitro.....	4
Figure 2.	Multipotency of mesenchymal stem cells.....	6
Figure 3.	YAP nuclear shuttling in response to mechanical challenge.....	8
Figure 4.	LIV device and cell culture plate placement.....	9
Figure 5.	(a) Clinostat simulated microgravity device redesign CAD model. (b) Clinostat shown inside incubator with 1 cell culture flask.....	11
Figure 6.	MATLAB image analysis process.....	13
Figure 7.	Acute LIV application increases nuclear YAP levels.....	20
Figure 8.	Basal nuclear YAP levels decreased by SMG were rescued by LIV.	21
Figure 9.	SMG and LIV application experimental design.....	22
Figure 10.	LIV _{AT} -induced YAP nuclear entry decreased by SMG was partially restored by daily LIV _{DT} application.....	23
Figure 11.	LPA addition increases nuclear YAP levels.....	25
Figure 12.	LPA-induced YAP nuclear entry decreased by SMG was not restored by daily LIV _{DT} application.....	26
Figure 13.	Nuclear stiffness and nuclear area size are not affected by SMG and SMG+LIV _{DT} treatments.....	28

LIST OF ABBREVIATIONS

LIV	Low Intensity Vibrations
AT	Acute LIV Treatment
DT	Daily LIV Treatment
YAP	Yes-associated Protein
MSC	Mesenchymal Stem Cells
SMG	Simulated Microgravity
LPA	Lysophosphatidic Acid
AFM	Atomic Force Microscopy

CHAPTER ONE: INTRODUCTION

1.1 Research Motivation:

The deterioration of the skeletal and muscular systems of astronauts on long-term space missions in microgravity and the resulting dramatically increased risk of traumatic physical injury is theorized to be due to the reduction of mechanical loading on the body and all of its musculoskeletal organs [1][2]. This process of dangerous bone and muscle atrophy is a result of the human body's mechanical adaptation mechanisms which remodel these tissues in order to maintain homeostasis. Various studies have begun to analyze the composition and characteristics of these mechanisms; however, their specific functional behavior remains incompletely understood. The identification and analysis of the components and their functions within these mechanisms may be instrumental in developing biomedical treatments capable of counteracting tissue atrophy like the conditions observed in long-term microgravity. The motivation for this research, therefore, was to reduce this knowledge gap by investigating the behavior of one of these signaling mechanisms.

1.2 Specific Experimental Goal

The YAP signaling pathway is one such signaling mechanism which has been identified and shown by studies to play a crucial role in the process of cell adaptation in response to mechanical stimulus [3][4]. In this pathway, the YAP protein is activated in response to mechanical stimulus and is shuttled into the cell nucleus where it activates

gene transcription leading to cell cycle entry and resulting in proliferation [5]. Our group and others have reported that simulated microgravity treatment applied to bone and muscle stem cells *in vitro* decreases proliferation of these cells which is necessary for healthy tissue regeneration [6][7]. Conversely, recent studies have shown that these stem cells display increased proliferative and differentiative responses to external mechanical stimuli, including applied mechanical vibration [8] and previous research from our group has demonstrated this treatment to be effective at countering the inhibitory effects of simulated microgravity on stem cell proliferation. Therefore, the specific goal of this research was to determine if the YAP signaling pathway is a contributing component of the mechanical adaptation mechanism which is responsible for the proliferation response of stem cells to simulated microgravity and mechanical vibrations. If this was found to be true, this research would seek to determine to what extent mechanical vibrations were able to alter and potentially counteract the inhibitory effects of simulated microgravity on YAP signaling.

CHAPTER TWO: BACKGROUND

2.1 Tissue Forces

2.1.1 Microgravity

The preservation and regeneration of healthy bone and muscle tissue which is necessary to maintain their mechanical integrity under physical loads is known to be impaired by microgravity. In general, this atrophy has been examined using simulated microgravity (SMG) and has been determined to be a result of decreased proliferation of the various cell types which make up the musculoskeletal tissues as well as decreased differentiation of multipotent stem cells into the required cell types. Specifically, for the skeletal system, bone tissue loss which results from unloading is a result of decreased generation of cell types including osteoblasts, osteocytes and adipocytes [9]. Muscular atrophy as caused by applied SMG is similarly a result of impaired myogenesis and proliferation of myoblasts and myocytes [10].

2.1.2 Low Intensity Vibrations

This form of muscle atrophy is a natural response to the elimination of mechanical forces exerted on bone and muscle tissues, a process which for the average human on Earth is counteracted at by constant mechanical forces which are experienced throughout the body. These forces include different kinds of strains regularly whether the human body is at rest or moving around. Forces experienced during movement and also at all times by gravity cause high magnitude strains in bones and muscles. In addition to these forces, high frequency contractions in our muscles cause low magnitude strains in

these tissues. Both of these kinds of forces are regularly experienced in healthy human body activity and both contribute to healthy bone and muscle tissue generation [11].

Recent research has developed mechanical treatments which are capable of simulating these crucial mechanical forces. Using various techniques, strain can be applied directly to the tissues to simulate the strains experienced during regular exercise [12].

Additionally, high frequency low magnitude strains can be simulated using low intensity vibrations (LIV) applied to organisms, to tissues, or even to cells individually both *in vivo* and *in vitro* as shown in **Figure 1** [13]. These mechanical treatments have been shown to activate and enhance tissue regeneration.

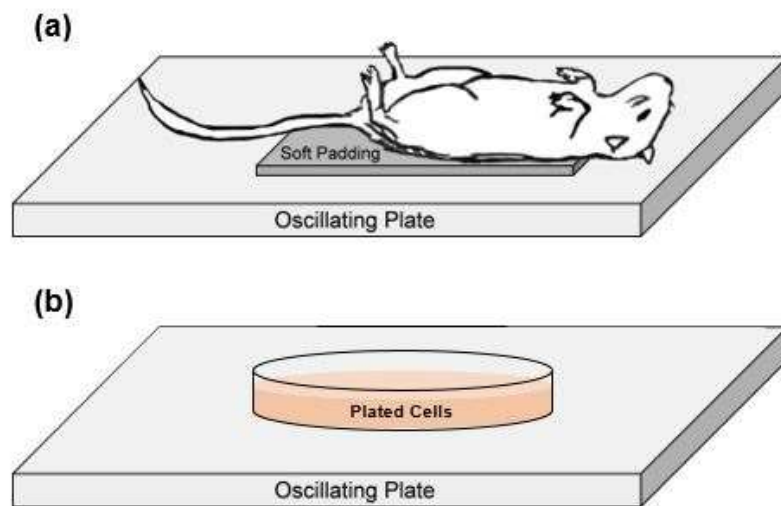


Figure 1. Application of low intensity vibrations (a) *in vivo* (b) *in vitro*.

2.2 Mechanoadaptive Regeneration

2.2.1 Cell Mechanoadaptation

These treatments rely on the mechanism which enables the tissues to be able to sense these forces and adapt appropriately. Studies have revealed that most eukaryotic cells are individually capable of sensing the forces in their environment. They respond with appropriate cell growth and development to form healthy tissues [14]. In order to sense these forces, they possess an elastic mechanical structure which is capable of deformation in response to these forces. The largest component of this mechanical structure is the cytoskeleton, which consists of actin fibers stretched between the cell membrane and the nucleus. The structure of the cytoskeleton, combined with the stiffness of the cell membrane and the nuclear membrane, enable the cell to deform under applied force. The resulting strain triggers the activation of various biochemical signaling pathways which initiate cell proliferation. This process by which cells respond to mechanical forces is known as mechanoadaptation. This process involves many specific biochemical components and many different signaling pathways. These pathways make up the mechanism which ensures healthy tissue growth via the process known as mechanoadaptation. As a result, they have been the subject of numerous studies, but many of these pathways are not yet completely understood. In order to take full advantage of the mechanoadaptation mechanism, these pathways and their components must be analyzed and fully defined.

2.2.1 Mesenchymal Stem Cells

All of the crucial cell types which make up musculoskeletal tissues share a common progenitor stem cell type: the mesenchymal stem cell (MSC). Therefore, the

active proliferation of MCSs both in response to mechanical stimulation and to unrelated signaling is required for the maintenance of the tissue integrity of musculoskeletal organs [6] as shown in **Figure 2**.

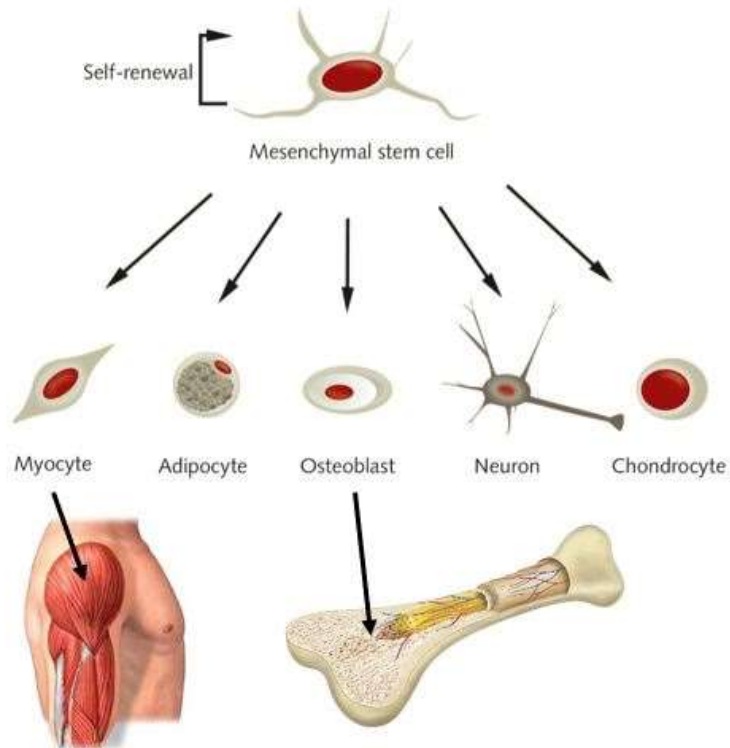


Figure 2. Multipotency of mesenchymal stem cells.

It is for this reason that MSCs have been identified as a key focus of tissue engineering research including studies attempting to describe the mechanical adaptation process of the muscular and skeletal systems. To be clear, MSCs and most animal cells possess this mechanoadaptive ability on the individual scale and can sense and adapt to mechanical forces even without connection to or interaction with other cells [15]. This indicates that the structural and signaling components which enable this process, including but not limited to the cytoskeleton, cellular and nuclear membranes, and the YAP signaling pathway, exist within each cell individually; therefore, these components

can be examined in vitro to observe their responses to mechanical stimulation applied directly to the cells.

2.3 Mechanoadaptive Signaling

2.3.1 Cell Signaling Pathways

Recent research has confirmed that MSC proliferation is decreased by applied SMG and has also demonstrated that this can be tested and observed in vitro [7]. This means that subcultured MSC's plated in flasks and subjected to mechanical stimulus, or lack thereof in the case of SMG, are capable of interpreting the stimulus in order to trigger an adaptive response. This phenomenon, in turn, points to a signaling pathway or coordinated mechanism consisting of signaling pathways which exist within each cell and is capable of translating mechanical stimulus into biochemical signals to trigger proliferation. This is further supported by other studies which have shown that MSCs display proliferative and differentiative responses to other mechanical conditions including but not limited to cell adhesion area [7][11], plating substrate stiffness [7][8], applied substrate strain [6], and applied low intensity vibrations (LIV) [6][16]. From these sets of data, it can be surmised that MSCs possess some mechanical structure which is capable of sensing the both passive and active mechanical conditions around them. The process by which MSCs as well as most animal cells sense and adapt to these conditions is generally referred to as mechanoadaptation. Considering this, both the mechanical structure and the signaling components involved in these processes work in conjunction to enable the mechanoadaptation mechanism of MSCs.

2.3.2 YAP Signaling Pathway

One such biochemical signaling pathway is the YAP signaling pathway. YAP (Yes-associated protein) is a signaling protein which is known to activate cell proliferation, or cell growth [3]. YAP signaling has been shown by many studies to be activated in response to the application of mechanical forces [6]. In the process of YAP signaling, YAP proteins move within a cell from the cytoplasm to the nucleus, where it activates gene transcription for cell proliferation, as shown in **Figure 3**. Recent research has shown that YAP signaling is required to activate proliferation in response to mechanical stimulation, meaning it is a critical component of the mechanoadaptation mechanism [6].

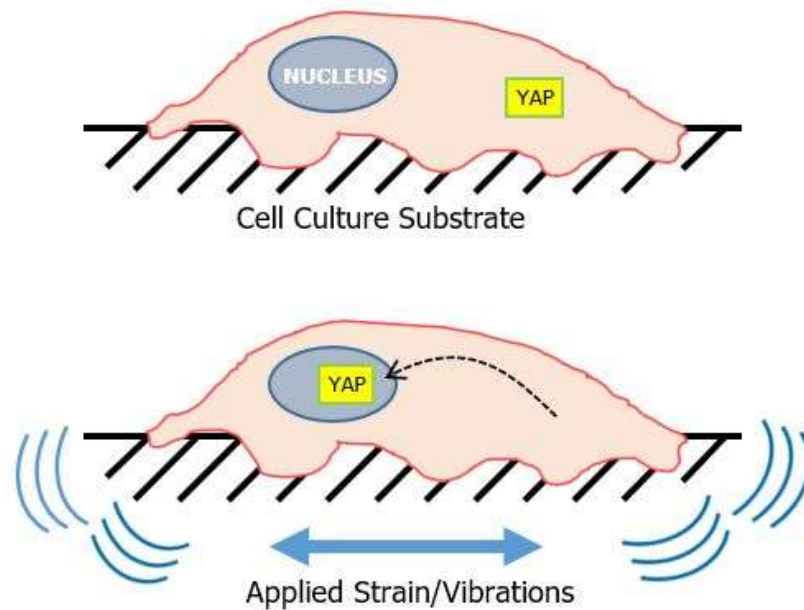


Figure 3. YAP nuclear shuttling in response to mechanical challenge.

CHAPTER THREE: DEVELOPMENT OF METHODS

3.1 Mechanical Treatments

3.1.1 Low Intensity Vibrations Treatment

LIV was to be applied to MSCs *in vitro* using a custom-made LIV device as described in previous research [7] as shown in **Figure 4**. This device was capable of vibrating MSCs plated in various kinds of tissue culture containers. The LIV device subjected cells to low intensity 90 Hz lateral vibrations at 0.7g for 20min intervals.



Figure 4. LIV device and cell culture plate placement.

In order to examine the effects of LIV treatment both in the form of long-term application and of acute single burst treatments, two separate LIV treatment protocols were developed. The first treatment was dubbed daily LIV treatment (LIV_{DT}) and was based on the treatment protocol developed previously in the lab which was able to counteract the effects of 72h of SMG on MSC proliferation [7]. This treatment was

applied for 3 days with 20min LIV sessions 2x per day separated by a 2h refractory period to enhance effects as demonstrated in previous research [17].

The alternate treatment protocol dubbed acute LIV treatment (LIV_{AT}) was developed to emulate acute mechanical treatment protocols which had been demonstrated by outside studies to be able to stimulate YAP signaling [6]. This treatment consisted of 5x 20min treatments with 1h in between each for a total of 340min (nearly 6h) total treatment time with the 1h pauses acting as refractory periods during this time. The plated cells were returned to the incubator during the refractory periods.

3.1.2 Simulated Microgravity Treatments

For the application of SMG, our lab had previously built a clinostat device which subjected MSCs plated in culture flasks to SMG by rotating them constantly at 15 RPM. This method of simulating microgravity works by constantly changing the vector of force due to gravity acting on the cells in order to effectively negate this force vector. A technical requirement of this method was that the flasks must be capable of being filled completely with cell medium and sealed with no bubbles, because these would be dragged across the MSCs while the flask was rotating and damage them. The initial design used for previous experiments in the lab [7] used airtight flasks to accomplish this, but this design was not suitable for immunofluorescence staining. To adapt the protocol to allow for this analysis, it was necessary to select a new kind of flask which allowed for both airtight sealing and also could be used for staining. The culture flask which was selected was the Nunc SlideFlask, which is comprised of an imaging slide with a flask section connected to it with airtight sealant. This also required that the clinostat SMG device be redesigned in order for it to be capable of holding these new flasks (**Figure 5a**).

For experiments, MSCs were plated in the SlideFlasks and secured in clinostat inside incubator which subjected them to SMG for 72h as shown in **Figure 5b**.

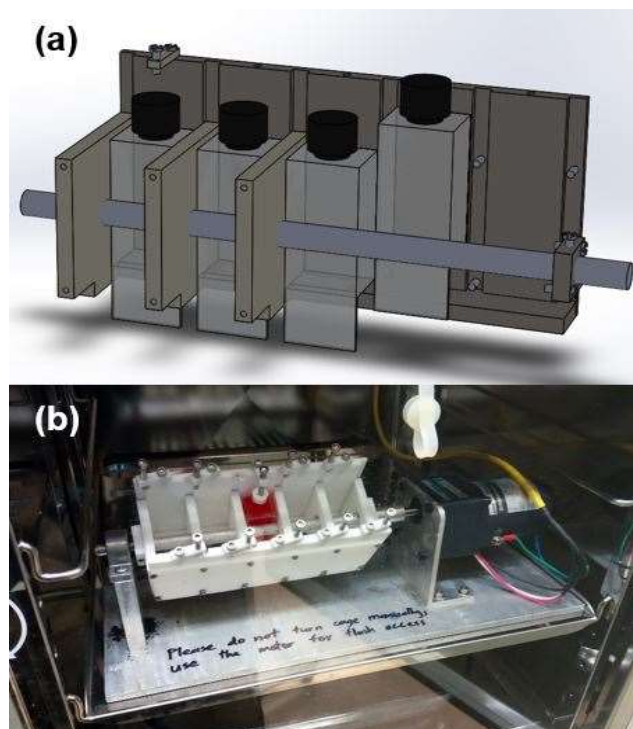


Figure 5. (a) Clinostat simulated microgravity device redesign CAD model. (b) Clinostat shown inside incubator with 1 cell culture flask.

3.2 Protein Tracking using Immunofluorescence Microscopy

3.2.1 YAP Immunofluorescence Staining

Immunofluorescence staining was used to track localization of the YAP proteins inside the experimental MSCs in order to quantify and analyze YAP nuclear shuttling. Following mechanical treatments, the flask sections of SlideFlasks were removed to access plated MSCs. These cells were stained with YAP specific antibody and fluorescent red secondary antibody and nuclear DNA was labeled via DAPI stain. Stained

samples were stored with protection from light to prevent photobleaching and imaged within a week to preserve stain quality.

3.2.2 Stained Sample Imaging

Stained samples were then imaged with laser scanning confocal microscopes to obtain images of stained cells for protein localization analysis. Two separate confocal microscopes were used, the first stage of experiments before the implementation of LPA application were imaged using a Leica TCS SP8, and following experiments were imaged using a Zeiss LSM 510 Meta; however, a 40x oil-immersion objective setup was used with both confocal microscopes, and all experiments contained individual image analysis normalized to control levels.

3.2.3 Image Analysis

Exported images were used to quantify relative YAP levels within each nuclei, with the nuclear regions traced by DAPI stained nucleus, which was accomplished using a custom-made Matlab code. The code worked by first separating the red and blue colored data from the YAP and DAPI stain respectively, then it identified the nuclear regions using the blue stain and isolated the stained YAP inside the nuclear regions as shown in **Figure 6**. The result was a list of red pixels for each cell nuclei which correspond to the concentration of YAP protein inside the nuclei. For each individual nucleus identified by the code, the average intensity of the pixels was found and stored as an individual data point. These average nuclear YAP protein stain intensity data points were subsequently all normalized to the control levels and presented on bar graphs in order to visualize the effects of mechanical treatments on YAP nuclear levels.

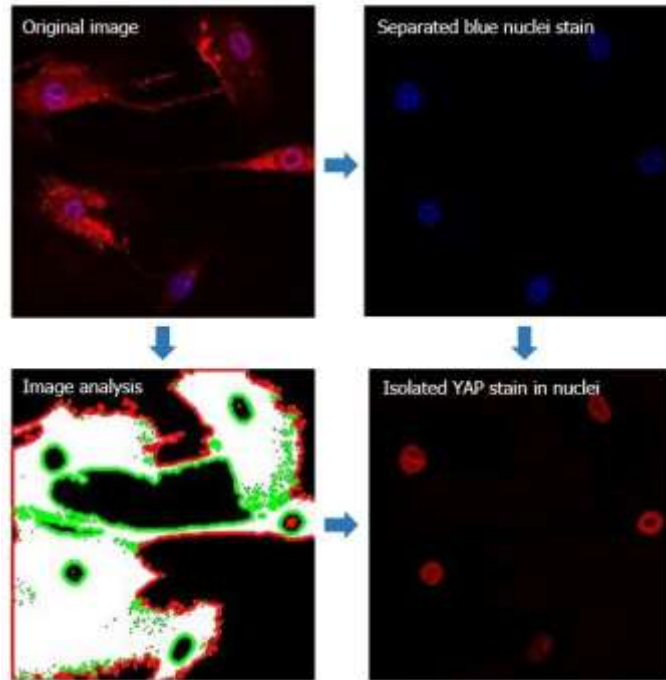


Figure 6. MATLAB image analysis process.

CHAPTER FOUR: MANUSCRIPT. “LOW INTENSITY VIBRATIONS RESTORE
NUCLEAR YAP LEVELS AND ACUTE YAP NUCLEAR SHUTTling IN
MESENCHYMAL STEM CELLS SUBJECTED TO SIMULATED MICROGRAVITY”

Thompson T¹, Woods K², Newberg, J¹, Uzer G¹ †

¹Mechanical and Biomedical Engineering, Boise State University

²Biomolecular Sciences Graduate Program, Boise State University

† **Corresponding Author**

Running title: LIV rescues SMG-inhibited YAP nuclear entry

Funding support: NASA ISGC NNX15AI04H and NIH 5P2CHD086843-03,
P20GM109095, and P20GM103408

† **Corresponding author:**

Gunes Uzer PhD

Boise State University

Department of Mechanical & Biomedical Engineering

1910 University Drive, MSd-2085

Boise, ID 83725-2085

Ph. (208) 426-4461

Email: gunesuzer@boisestate.edu

4.1 Abstract

The bone deterioration that astronauts experience in microgravity environments is known to occur in response to the lack of gravity-based tissue stress. Mechanical forces are crucial to maintain healthy bone mass by regulating the function of bone-making osteoblasts as well as the proliferation and differentiation of their progenitors, mesenchymal stem cells (MSC) which replenish osteoblastic cells. Regulation of proliferative function of MSCs in response to mechanical force is in part controlled by the “mechanotransducer” protein YAP (Yes-associated protein) which is shuttled into the nucleus in response to mechanical challenge to induce gene expression necessary for cell proliferation. Our group had recently reported that altered gravity conditions under simulated microgravity (SMG) decreases proliferation of MSCs and that application of daily low intensity vibrations (LIV) during SMG reverses this effect on proliferation. While these findings suggest that LIV may be a promising countermeasure for altered loading, the specific SMG and LIV effects on YAP mechanosignaling are unknown. Therefore, here we tested the effects of SMG and daily LIV treatment on basal nuclear YAP levels as well as on the acute YAP nuclear entry in response to both mechanical and soluble factors in MSCs. MSCs subjected to 72h of SMG, despite decreased nuclear YAP levels across all groups, responded to both LIV and Lysophosphohaditic acid (LPA) treatments by increasing nuclear YAP levels within 6hrs by 49.52% and 87.34%, respectively. Additionally, daily LIV restored the basal decrease seen in SMG as well as nuclear YAP levels as well as restored in part the YAP nuclear entry response to subsequently applied acute LIV and LPA treatments. These results show that rescue of basal YAP levels by LIV may explain previously found proliferative effects of MSCs

under SMG and demonstrates that daily LIV is capable of alleviating the inhibition caused by SMG of YAP nuclear shuttling in response to subsequent mechanical and soluble challenge.

4.2 Introduction

The musculoskeletal deterioration which astronauts experience on long-term space missions and the resulting increase of traumatic physical injury risk is in-part due to the reduction of mechanical loading on the musculoskeleton [18][19]. This process of dangerous bone and muscle atrophy is a result of the human body's mechanical adaptation mechanisms which remodel these tissues in order to maintain homeostasis under mechanical challenge. To alleviate the detrimental effects of unloading, astronauts undergo long intensive regimens of running and resistance training in orbit [18]. Despite these efforts, astronauts lose an average bone density of 1% for each month they spend in space [1][19]. This loss necessitates new non-pharmacologic therapies in addition to exercise to keep bones healthy during long-term space missions. In bone, tissue level response to mechanical challenge is in-part regulated by osteoblasts and osteocytes [20]. Both osteoblasts and osteocytes in turn share a common progenitor: the mesenchymal stem cell (MSC). Therefore, the growth and differentiation of MSCs in response to mechanical stimulation is required for the maintenance and repair of bone [21]. It is for this reason that MSCs are a potential target for mechanical therapies aiming to alleviate bone loss in astronauts, service personnel with long periods of bedrest, and physically inactive aged individuals [22].

To maintain healthy bone making cell populations, MSCs rely on environmental mechanical signals inside the bone marrow niches near bone surfaces. While the exact

characteristics of the mechanical environment that MSCs exist in remain to be quantified, it is known that during habitual activities our bones are subjected to combinations of complex loads including strain, fluid shear, and accelerations, each of which is inseparable [23]. For example, during moderate running, cortical bone can experience strains up to $2000\mu\epsilon$ [24][25], which also generate coupled fluid flow within canaliculi up to $100\mu\text{m/s}$ [26]. The interior of bone is filled with bone marrow with viscosities up to $400\text{-}800\text{cP}$ [27]. During moderate running, tibial accelerations reach to $2\text{-}5\text{g}$ range [28] ($1\text{g} = 9.81 \text{ m/s}^2$), creating a complex loading at the bone-marrow interface that depends on many factors including frequency, amplitude, and viscosity [29]. In silico studies reveal that when exposed to vibrations ($0.1\text{-}2\text{g}$), marrow-filled trabecular compartments generate fluid shear stresses up to 2Pa [29][30], capable of driving bone cell functions [31]. Interestingly, while these high magnitude forces are only experienced a handful of times during the day, bones are bombarded by smaller mechanical signals arising from muscle contractions that generate bone strains ranging between 2 to $10\mu\epsilon$ [11].

Exogenous application of these small magnitude mechanical regimes in the form of low intensity vibrations (LIV) ranging between $0.1\text{-}2\text{g}$ acceleration magnitudes and $20\text{-}200\text{Hz}$ frequencies were shown to be effective in improving bone and muscle indices in clinical and preclinical studies [32]. At the cellular level our group has reported that application of LIV increases MSC contractility [8], activates RhoA signaling [16], and results in increased osteogenic differentiation and proliferation of MSCs [7][33].

One of the most studied signaling pathways that regulate the MSC mechanoresponse is the Yes-associated protein (YAP) signaling pathway. As evidence of the contributing role of YAP in cell proliferation and growth, YAP depletion in stem cells

results in reduced proliferation and osteogenesis [4][34]. Similarly, depleting YAP from osteoblast progenitors decreases both bone quality and quantity in mice [35].

Functionally, in response to cytomechanical forces and substrate stiffness, YAP moves from the cytoplasm to the nucleus where it interacts with its co-transcriptional activators such as TEAD to regulate gene expression related to proliferation [36]. For example, application of substrate strain induces YAP nuclear entry and YAP transcriptional activity which is required to activate proliferation [5]. While it has been shown that YAP nuclear entry is triggered by soluble factors increasing F-actin contractility such as Lysophosphatidic acid (LPA) [37][38], large changes in substrate stiffness [4], or substrate stretches ranging from 3% to 15% [5][6], it is not known if low magnitude signals like LIV also trigger acute YAP nuclear entry.

Research aimed at studying the effects of microgravity at the cell level often relies on simulated microgravity (SMG) devices designed to alter the gravitational conditions that cell experience by rotating on one or multiple axis at low speeds [39][40][41]. Research from our group and others show that SMG results in reduced cytoskeletal contractility [39][42][43] and reduced levels of integral nuclear proteins such as Lamin A/C and LINC (Linker of Nucleoskeleton and Cytoskeleton) complex element Sun-2. Concomitantly, applied SMG also consistently results in decreased MSC proliferation. To test the efficacy of LIV as a possible countermeasure for sMG-induced proliferation loss, we have shown that twice daily application of LIV for 20 minutes during 72h SMG was able to recover MSC proliferation levels as well as the reduced levels of nuclear envelope proteins [7]. As mechanically induced YAP nuclear shuttling has been associated with

LINC complex function [44], these findings suggested that SMG should serve to decrease YAP nuclear entry in response to mechanical or soluble factors.

Therefore, here we set out to answer the hypothesis SMG-induced impairment of acute YAP nuclear entry in response to mechanical and soluble factors will be alleviated by daily application of LIV.

4.3 Results

4.3.1 Acute LIV Application Increases Nuclear YAP Levels

To quantify the acute YAP nuclear entry in response to LIV, MSCs were plated at the density of 1,700cells/cm² and were allowed to attach for 24hr. Following this, MSCs were subjected to treatment in two groups: control and acute LIV treatment regimen (LIV_{AT}). The LIV_{AT} regimen consisted of 5x 20min vibration periods separated by 1hr in between each at room temperature while control samples were also taken out of the incubator but were not vibrated. Immediately after LIV_{AT}, the samples stained against YAP and DAPI were imaged, followed by MATLAB image analysis to quantify the changes in the nuclear YAP levels. As shown in **Figure 7a**, qualitative visual analysis of the resulting images showed an increase in YAP staining in the cell nuclei. Analysis shown in **Figure 7b** revealed a 32.43% increase in the nuclear YAP levels of the LIV_{AT} samples as compared to the control samples ($p < 0.0001$). As both LIV-induced focal adhesion signaling [16] and YAP nuclear entry in response to substrate strain [6] requires intact LINC function, disabling LINC function via a dominant negative overexpression of Nesprin KASH (Klarsicht, ANC-1, Syne homology) fragment (DNK) both decreased basal nuclear YAP levels by 33.91% ($p < 0.0001$) and reduced the LIV-induced YAP nuclear entry when compared to empty plasmid (**Figure S1**).

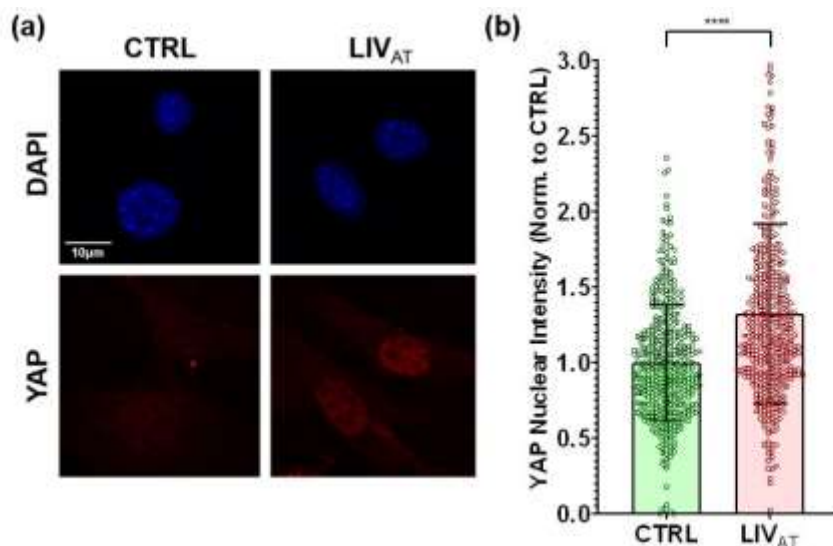


Figure 7. Acute LIV application increases nuclear YAP levels.

(a) MSCs were subjected to LIV_{AT} and stained with DAPI and YAP red. Images showed LIV_{AT} increased nuclear YAP levels as well as overall cellular levels. (b) MATLAB analysis revealed LIV_{AT} samples 32.43% increase in nuclear YAP levels compared to control levels. $n > 400/\text{grp}$, group comparison was made a Mann-Whitney post-hoc test, ** $p < 0.0001$.**

4.3.2 Basal Nuclear YAP Levels Decreased by SMG Were Rescued by LIV

We next tested whether a daily LIV treatment regimen (LIV_{DT}), applied in parallel with SMG, could alleviate basal YAP levels in the nucleus. As we reported previously, LIV_{DT} consisted of 2x 20min vibrations every 24 hours during the 72h period of SMG application which was effective at restoring MSC proliferation and the whole cell YAP levels when applied in conjunction with SMG [7]. MSCs were plated at the density of 1,700cells/cm² in 25cm² tissue culture SlideFlasks (Nunc, #170920) and were allowed to attach for 24h, after which point the flasks were filled completely with growth medium, sealed, and subjected to 72h of treatment followed by staining against YAP and DAPI. During the 72h treatment period, MSCs were divided into three groups: control samples, SMG samples which were subjected to the standard regimen of 72h of continuous SMG, and SMG+LIV_{DT} samples which were subjected to both the 72h SMG

regimen and the daily LIV_{DT} regimen. Representative images for YAP and DAPI stained images are shown in **Figure 8a**. As depicted in **Figure 8b**, MATLAB analysis revealed a 41.60% decrease in the nuclear YAP intensity of the SMG samples as compared to the control samples ($p < 0.0001$). Compared to the SMG group, nuclear YAP levels of the LIV_{DT} treated MSCs showed an increase of 66.75%, respectively. There was no significant nuclear YAP level difference between of LIV_{DT} treated MSCs and non-SMG controls.

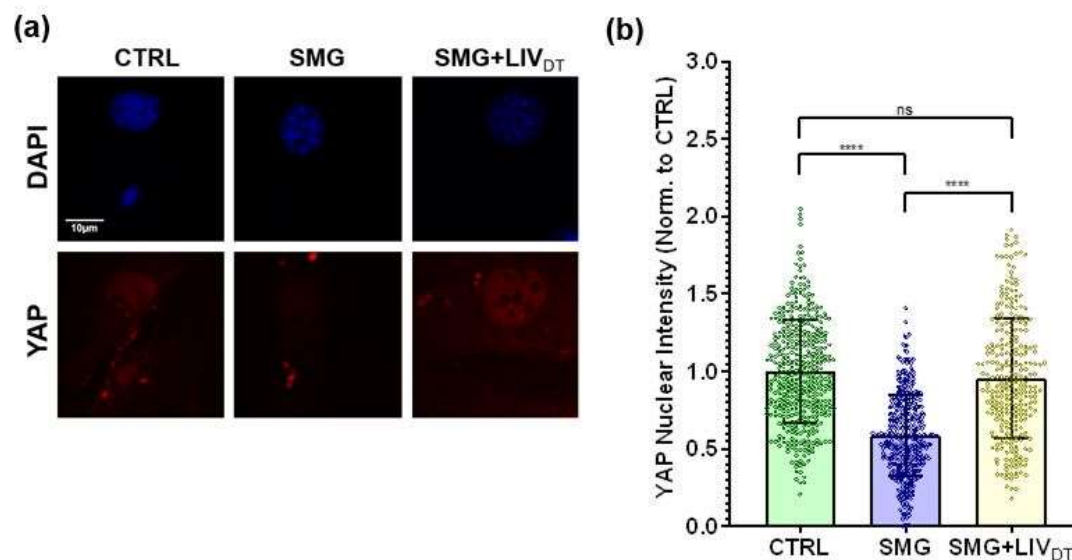


Figure 8. Basal nuclear YAP levels decreased by SMG were rescued by LIV. (a) MSCs were subjected to SMG, and SMG+LIV_{DT} over 72h period and stained with DAPI and YAP red. **(b)** MATLAB analysis showed for SMG sample 41.60% decrease of nuclear YAP levels compared to control levels. Combined SMG+LIV_{DT} treatment samples showed 66.75% increase of nuclear YAP levels with compared to SMG samples to no significant difference with control levels. $n > 100$ /grp, group comparisons were made using one-way ANOVA, **** $p < 0.0001$.

4.3.3 LIV_{AT}-induced YAP Nuclear Entry Decreased by SMG Was Partially Restored by Daily LIV_{DT} Application

As SMG decreased basal nuclear YAP levels, we next tested whether SMG decreases LIV_{AT}-induced YAP mechanosignaling (i.e. nuclear shuttling). Since LIV_{DT}

was able to restore nuclear YAP levels (**Figure 8**), the SMG+LIV_{DT} group was added to evaluate the effect of LIV_{DT} on the SMG response. A schematic of the experimental design is given in **Figure 9**.

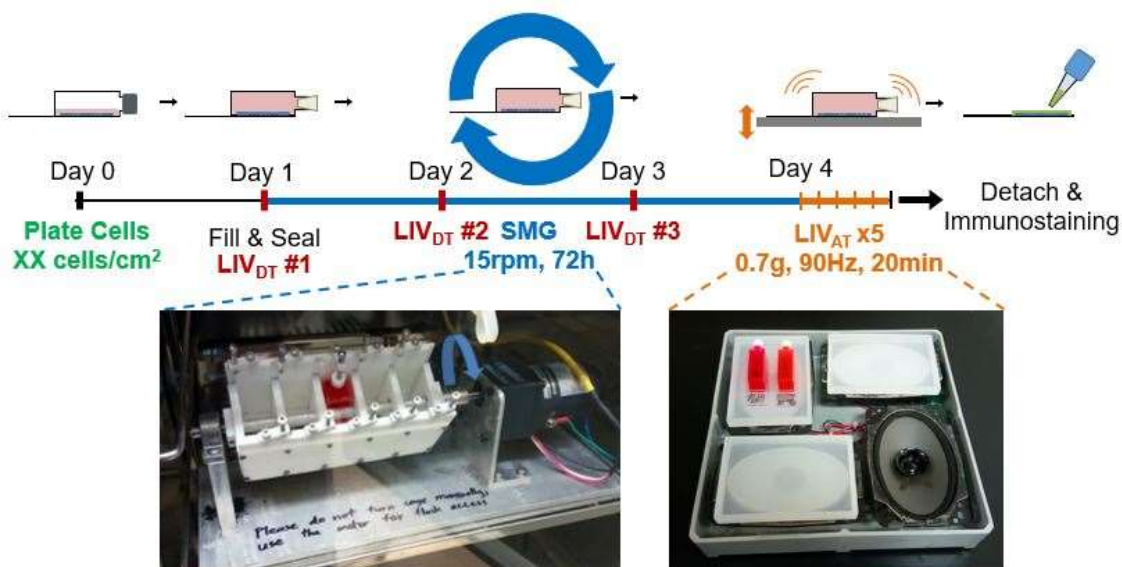


Figure 9. SMG and LIV application experimental design.

MSCs were subcultured and plated in SlideFlasks and allowed to attach for 24h before SlideFlasks were filled with culture medium and sealed for mechanical treatments. After treatment, flask was removed to isolate the cells on slide for immunofluorescence staining. Treatment regimen for MSC's involved 72h SMG with additional LIV and/or LPA application as shown. LIV_{DT} regimen consisted of one treatment cycle every 24hr during SMG treatment with each cycle consisting of 2x 20min LIV with an hour in between. LIV_{AT} regimen was applied after 72h SMG treatment period and consisted of 5x 20min LIV with an hour in between each. For LIV application, MSCs plated in Slideflasks were placed in LIV device constructed in the lab previous to this research. Vibrations were applied at peak magnitudes of 0.7 g at 90 Hz at room temperature. For SMG application, MSCs plated in SlideFlasks were secured in lab custom-built clinostat inside incubator. The clinostat subjected the MSCs to constant 15 RPM rotation simulated microgravity.

MSCs were divided into six groups where the CTRL, SMG, SMG+LIV_{DT} groups were treated with \pm LIV_{AT} at the end of 72h and nuclear YAP levels were measured. Similar to previous experiments, SMG alone decreased basal nuclear YAP levels by 36.99% ($p < 0.0001$) which were increased back to control levels in the SMG+LIV_{DT}

group. As depicted in **Figure 10**, +LIV_{AT} increased nuclear YAP levels in the CTRL, SMG and SMG+LIV_{DT} groups by 49.52%, 69.01% and 21.87%, respectively ($p < 0.0001$) while exhibiting the smallest increase in the SMG+LIV_{DT}. As a result, final nuclear YAP levels in the SMG+LIV_{DT}+LIV_{AT} group remained not significantly different from the SMG+LIV_{AT} and 22.60% smaller than the LIV_{AT} group.

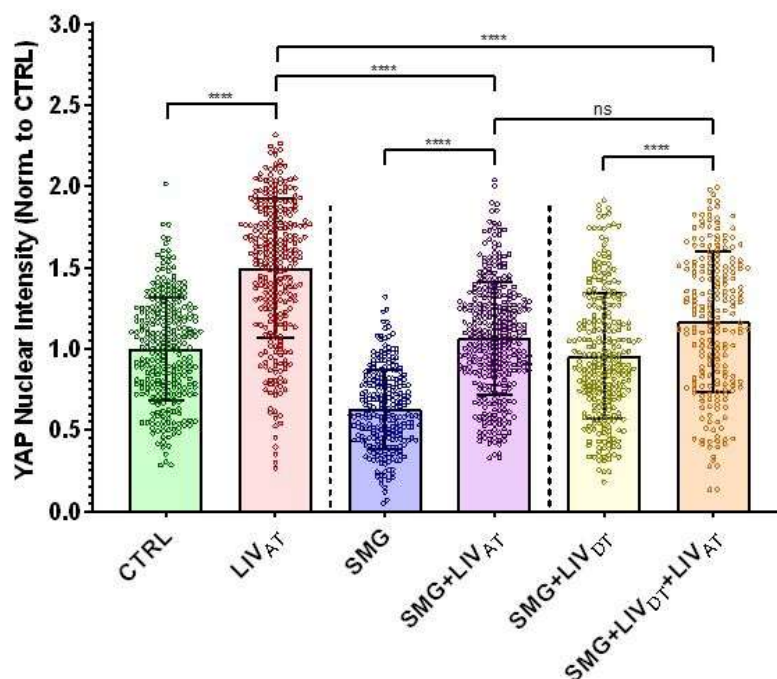


Figure 10. LIV_{AT}-induced YAP nuclear entry decreased by SMG was partially restored by daily LIV_{DT} application.

MSCs were subjected to SMG, and parallel SMG+LIV_{DT} over 72h period, shown in first, third, and fifth columns. Additional experiments examined YAP nuclear entry sensitivity to LIV_{AT} application of these three samples, shown in second, fourth, and sixth columns. MATLAB analysis of stained images revealed sensitivity of CTRL sample to be 49.52%, of SMG sample to be 77.12%, and of SMG+LIV_{DT} sample to be only 21.87%. MATLAB analysis also showed for SMG+LIV_{AT} samples 29.18% decrease and for SMG+LIV_{DT}+LIV_{AT} samples 22.60% decrease of LIV_{AT}-induced YAP nuclear entry compared to LIV_{AT} samples. $n > 200/\text{grp}$, group comparisons were made using one-way ANOVA, **** $p < 0.0001$.

4.3.4 LPA Addition Increases Nuclear YAP Levels

As LIV_{DT} treatment did not restore the acute LIV_{AT} response to that of control levels, we next considered a soluble regulator of cytoskeletal tension, LPA. To test the effect of LPA on the acute YAP nuclear entry, two LPA concentrations (50 μ M and 100 μ M) were compared against control samples. Shown in **Figure 11**, nuclear YAP levels were almost doubled under two hour exposure to 50 μ M LPA and 100 μ M LPA treatments with 98.55% and 106.52% increases as compared to the control samples ($p < 0.0001$). Nuclear Yap levels for 50 μ M LPA and 100 μ M LPA treatments were not significantly different.

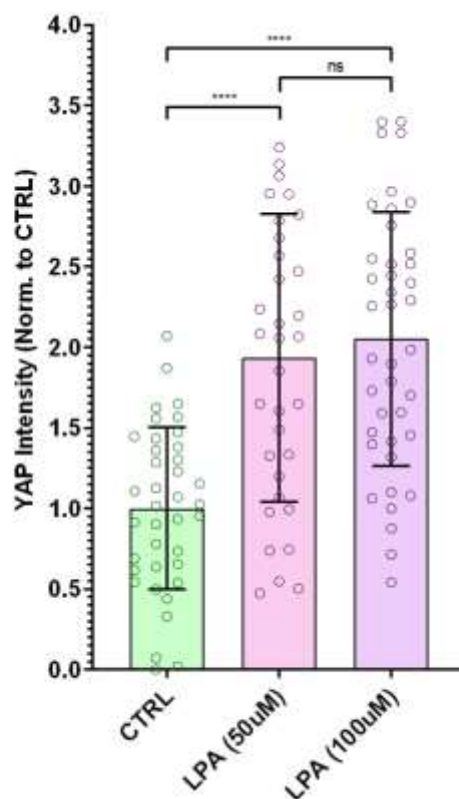


Figure 11. LPA addition increases nuclear YAP levels.

MSCs were subjected to LPA addition at 50uM and 100uM concentrations. MATLAB analysis of stained images revealed for LPA (50uM) samples 98.55% increase, and for LPA (100uM) samples 106.52% increase of nuclear YAP levels compared to control levels with no significance difference between the concentrations. $n > 30/\text{grp}$, group comparisons were made using one-way ANOVA, **** $p < 0.0001$.

4.3.5 LPA-induced YAP Nuclear Entry Decreased by SMG Was Partially Restored by Daily LIV_{DT} Application

In order to evaluate whether LIV_{DT} can restore LPA-induced YAP mechanosignaling (i.e. nuclear shuttling) after SMG, 50uM LPA or DMSO were added to the samples at the end of the 72h treatment of either CTRL, SMG or SMG+LIV_{DT} treatments. The CTRL group, SMG group, and SMG+LIV_{DT} groups were subjected to the same treatment as in the previous experiments and displayed similar results. As depicted in **Figure 12**, +LPA increased nuclear YAP levels in the CTRL, SMG and

SMG+LIV_{DT} groups by 104.78%, 66.63% and 43.39% respectively ($p < 0.0001$). While final YAP nuclear levels in SMG+LIV_{DT}+LPA remained higher than the CTRL and SMG+LPA groups ($P < 0.0001$), they remained 29.05% smaller than the LPA group.

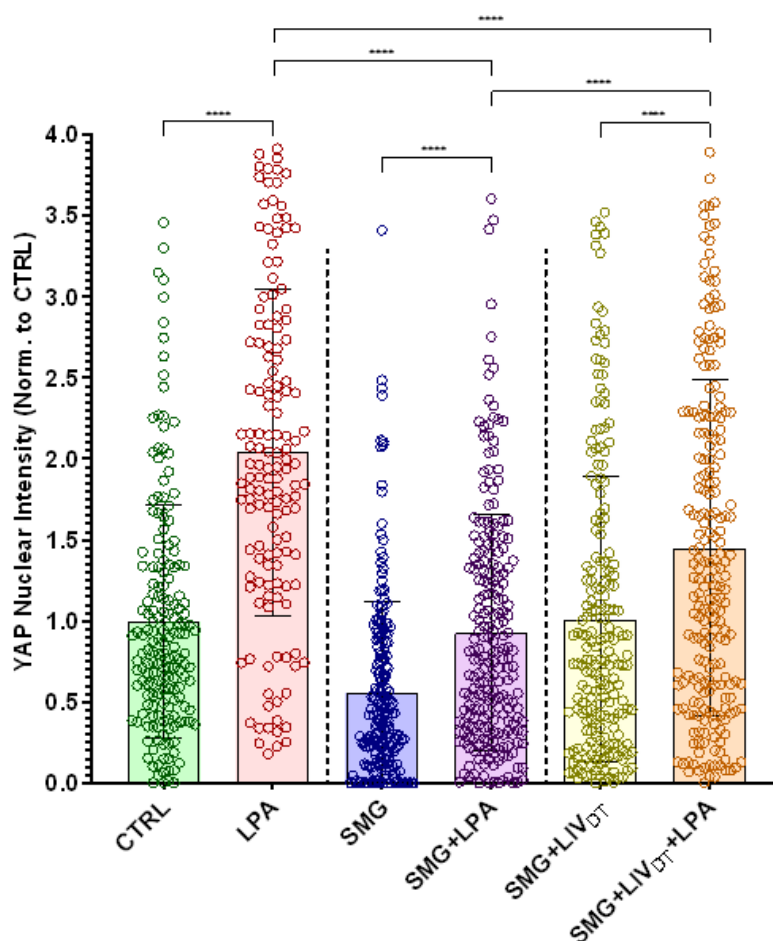


Figure 12. LPA-induced YAP nuclear entry decreased by SMG was not restored by daily LIV_{DT} application.

MSCs were subjected to SMG, and parallel SMG+LIV_{DT} over 72h period, shown in first, third, and fifth columns. Additional experiments examined YAP nuclear entry sensitivity to LPA addition of these three samples, shown in second, fourth, and sixth columns. MATLAB analysis of stained images revealed sensitivity of CTRL sample to be 104.78%, of SMG sample to be 66.63%, and of SMG+LIV_{DT} sample to be only 43.39%. MATLAB analysis also showed for SMG+LPA samples 55.17% decrease and for SMG+LIV_{DT}+LPA samples 29.05% decrease of LPA-induced YAP nuclear entry compared to LPA samples. MSCs subjected to SMG, and parallel SMG+LIV_{DT} over 72h period. Experiments examined sensitivity to LPA of these three samples. $n > 100/\text{grp}$, group comparisons were made using one-way ANOVA, **** $p < 0.0001$.

4.3.6 SMG and LIV_{DT} Do Not Affect Nuclear Stiffness or Nuclear Area

As YAP mechanosignaling of SMG+LIV_{DT} MSCs remained below control levels in response to both LIV_{AT} and LPA, we quantified the nuclear stiffness in CTRL, SMG and SMG+LIV_{DT} samples. AFM Testing was used to quantify the elastic modulus of the nucleus by measuring load-displacement curves on top of the nucleus. As shown in **Figure 13a**, analysis revealed no statistically significant effect on nuclear elastic modulus in the SMG or SMG+LIV_{DT} groups compared to control levels. We have further quantified nuclear area as a measure of cyto-mechanical forces on the nucleus [45]. Shown in **Figure 13b**, analysis of cross-sectional area of cell nuclei using DAPI stained images revealed no significant effects on average nuclear size by either SMG or combined SMG+LIV_{DT} treatment compared to control levels.

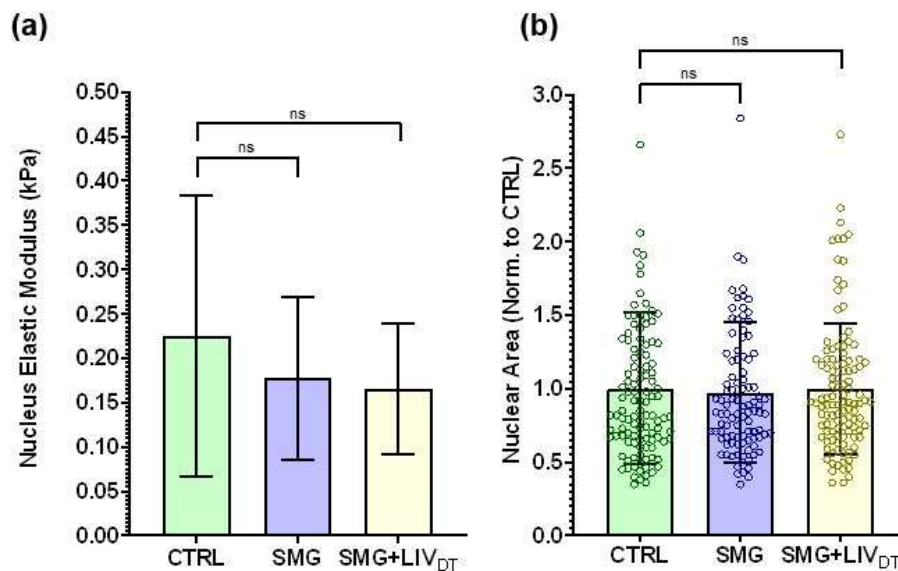


Figure 13. Nuclear stiffness and nuclear area size are not affected by SMG and SMG+LIV_{DT} treatments.

MSCs were subjected to SMG, and parallel SMG+LIV_{DT} over 72h period. (a) AFM analysis of live cells revealed apparent 21.09% decrease and SMG+LIV_{DT} samples showed similar apparent decrease of nuclear membrane elastic modulus to 26.57% below control levels, however statistical analysis revealed these changes to not be statistically significant. $n=10/\text{grp}$, ns, $p=0.8713$, against control levels. (b) MATLAB image analysis of the same treatment groups revealed no significant effects of either SMG or LIV treatment on the average nucleus size. $n=100/\text{grp}$, group comparisons were made using one-way ANOVA, ns, $p=0.5103$.

4.4 Discussion

The mechanical forces to which the bone and muscle tissue cells of the human body are subjected both on Earth and in microgravity environments are complex and remain incompletely understood. At the same time, it is clear that these forces are required for healthy tissue growth on Earth and are adversely affected in microgravity which is the cause of tissue degeneration. The complexity of these forces makes it difficult to design realistic experiments that comprehensively simulate in vivo conditions. While the in vitro experiments utilizing SMG and LIV treatments used in this study are limited in this way and do not entirely correlate with the physiological behavior of these

cells in vivo, the experiments presented here remain useful for testing cell behavior under well-defined conditions.

In this study, the investigation of MSC mechanosignaling was focused on the YAP signaling pathway and the first step to characterize and define the effects of LIV on MSC YAP signaling capability was to develop and verify a method capable of analyzing MSC nuclear YAP levels and transient YAP nuclear entry response, specifically as they are affected by acute LIV or LPA treatments. The first experiments demonstrated that LIV application over several hours was capable of stimulating YAP entry into the nucleus (**Figure 7**). However, the later experiments called into question the suitability of LIV as treatment form of acute mechanical challenge, in particular after it had already been used for daily treatments.

In other studies, high magnitude applied mechanical strain has been used for this kind of treatment [5][6]. Because the application of real mechanical stretch treatment to the MSCs would have been very difficult to incorporate into the methods developed for simultaneous SMG and LIV application, LPA addition served as the best option for applying a simple mechanical stimulation in order to evaluate the YAP mechanotransduction. LPA is a phospholipid derivative signaling molecule which is capable of causing the simulation of static transient stretch of a cell by increasing the contractility of the cytoskeleton [33][46]. The first experiments with LPA served to verify that the simulation of stretch via increased cytoskeleton contractility was capable of triggering YAP entry into the nucleus and the analysis methods were capable of picking up this response (**Figure 11**).

In these and in the following experiments, MSCs in the various samples were observed visually to be at different life cycle stages and some were also potentially in the process of differentiation. It was for this reason that substantially large sample sizes were used for all experiments in order to accurately observe the authentic effects of the mechanical treatments. Additionally, levels of differentiating MSCs were expected to be low due to un-altered cell growth medium used and limited 72h treatment timespan for experiments; therefore, the effects of differentiation on nuclear YAP levels were assumed to be negligible.

The first SMG experiments confirmed a clear decrease in basal nuclear YAP levels. Interestingly, SMG treated cells remained highly responsive to mechanical and soluble activator of YAP nuclear entry as both LIV_{AT} and LPA treatments were able to raise the acute nuclear YAP levels back up to and above non-treated controls. However, YAP levels remained significantly below non-SMG groups (**Figures 8, 10 & 12**). These finding suggested that the YAP mechanosignaling apparatus of MSCs was to some extent intact under SMG. When applied in parallel to SMG, daily LIV_{DT} treatment was able to restore basal YAP levels in the cell nucleus (**Figure 8**) up to after 24h after the final LIV_{DT} treatment. As acute increases in YAP nuclear levels in response to mechanical challenge are shown to be transient [5] and expected to return to baseline after 24h, this increase in nuclear levels supported our earlier report that showed sustained recovery of MSC proliferation by LIV_{DT} [7].

Interestingly, this increase of basal nuclear YAP levels under LIV_{DT} was accompanied by a reduced MSC response to acute stimulations by both LIV_{AT} and LPA. While these levels were still restored to greater than SMG sample levels and greater than

initial control levels, they were only partially restored to the control plus acute treatment samples. This suggested that after the combined treatment period of SMG and LIV_{DT} to restore the nuclear YAP levels, there may have been some effect on the mechanosignaling mechanism which was limiting the sensitivity of the MCSs to additional mechanical stimulus. Initially, after analysis of the SMG+LIV_{DT}+LIV_{AT} samples, this was theorized to be due to LIV's potentially poor suitability as an treatment form of acute mechanical challenge (**Figure 10**); however, when LPA addition was tested in the role as the acute treatment, the same trend revealed that SMG had some effect on the mechanism which LIV_{DT} was not completely able to alleviate. At this point, additional experiments would be required to determine which component or components in the mechanism were affected. Data from previous research in our lab using the same treatment protocols as in these experiments suggested that total cellular YAP levels decreased by SMG were restored to control levels by daily LIV [7]. This would indicate that total availability of YAP in both the cytoplasm and the nucleus is not responsible for this observed incomplete restoration of YAP signaling response.

In regard to other potential effects of SMG on the components of the mechanosignaling mechanism, one current prevailing hypothesis considering YAP mechanosignaling in particular suggests a role of nuclear pore opening in response to cyto-mechanical forces [44] which may be affected by changes in the nuclear stiffness. Unfortunately, AFM experiments and additional YAP nuclear entry experiments were not able to identify any statistically significant effects of SMG or LIV_{DT} treatment on nuclear stiffness or on nuclear area (**Figure 13**). While future studies are required, considering the significant role which the nuclear membrane plays as a mechanical structural

component in the cell's interpretation of mechanical stimulus [47][48], our results were not able to detect any changes in nuclear stiffness may not be a factor in reduced YAP mechanosignaling after LIV_{DT} treatment of MSCs subjected to SMG.

In summary, while the restoration of basal nuclear levels under daily LIV_{DT} treatment suggest that LIV acts as a possible countermeasure to improve MSC response to detrimental effects of simulated microgravity, future studies are required to understand why acute YAP nuclear entry in response to mechanical and soluble factors remain less responsive.

4.5 Methods

4.5.1 Mesenchymal Stem Cell Culture

Primary mice bone marrow derived MSC's were extracted as previously described. MSCs were then subcultured and plated in Iscove modified Dulbecco's cell culture medium (IMDM, 12440053, Gibco) with 10% fetal calf serum (FCS, S11950H, Atlanta Biologicals) and 1% pen/strep. MSCs were subcultured every one week, stock cells were plated in 10cm culture dishes at a density of 1,300cells/cm², and experimental cells were plated in SlideFlasks at density of 1,700cells/cm² and given 24h to attach to the slide before being used for experiments. Cell passages for MSCs used for experiments were limited to P7-P15.

4.5.2 Low Intensity Vibrations Treatment

SlideFlasks with plated MSCs were filled completely with culture medium and placed in LIV device designed and used in previous research (**Figure 9**) [7]. LIV device subjected cells to low intensity 90 Hz lateral vibrations at 0.7g at room temperature. MSCs were vibrated for 20min intervals broken up over time. End treatment LIV

regimen was applied after 72h treatment period and consisted of 5x 20min LIV with an hour in between each. Daily treatment LIV regimen consisted of 3x treatments in parallel with SMG treatment each consisting of 2x 20min LIV with 2h in between.

4.5.3 Simulated Microgravity Treatment

SlideFlasks (Nunc, #170920) with plated MSCs were filled completely with culture medium (**Figure 9**) and placed in clinostat SMG device. The clinostat shown is a redesign of custom-made clinostat described in previous research [7]. with new flask holder casing capable of holding SlideFlasks and also is autoclavable. The clinostat subjected the MSCs to constant 15 RPM sMG for 72h.

4.5.4 Immunofluorescence Staining and Image Analysis

Immediately after mechanical treatment, MSCs plated in Slideflasks were removed from treatment, and the SlideFlasks were separated in order to stain the MSCs on the slides (Fig.3). The MSCs were fixed with 4% paraformaldehyde, then washed and permeabilized with 0.05% Triton X-100 in PBS, then immunostained with YAP specific antibody (YAP (D8H1X) Rabbit mAb, Cell Signaling Technologies) and Alexa Fluor red secondary antibodies (Donkey anti-Rabbit IgG (H+L) Cross-Adsorbed Secondary Antibody, Alexa Fluor Plus 594 for all experiments prior to usage of LPA, after this Donkey anti-Rabbit IgG (H+L) Cross-Adsorbed Secondary Antibody, Alexa Fluor Plus 633 was used). Nuclear DNA was labeled via DAPI (Vectashield Mounting Medium, Vector Laboratories). Cytoskeletal actin was labeled using Phalloidin in (Alexa Fluor 488 Phalloidin- Invitrogen). Stained samples were imaged with confocal microscope (Leica TCS SP8 confocal microscope, 40x, HC PL APO CS2 Oil Immersion, 1024x1024 .jpg images prior to usage of LPA, after this Zeiss LSM 510 Meta Confocal Microscope, 40x,

HC PL APO CS2 Oil Immersion, 1024x1024 .jpg was used). Exported images were used to quantify relative YAP levels within each nuclei (nuclear regions traced by DAPI stained nucleus) via custom-made MATLAB program (The MathWorks, Natick, MA). DAPI images were analyzed using an edge-detection algorithm in order to determine the nuclear area for each cell. The nuclear outline was then used as a mask to quantify the average pixel intensity of the YAP stain within the nuclei of each individual cell. (n=50-100 nuclei/sample).

4.5.3 Atomic Force Microscopy

Bruker Dimension FastScan AFM was used for collection of the atomic force measurements. Tipless MLCT-D probes with a 0.03 N/m spring constant were functionalized with 10 μm diameter borosilicate glass beads for force collection. The AFM's optical microscope was used to locate individual live MSCs plated on the SlideFlask slides but with the flask section removed for access to the cells. The nucleus of each cell was tested with at least 3 seconds of rest between each test. In each test, three force-displacement curves were obtained (ramping rate: 2 $\mu\text{m}/\text{sec}$ over 2 μm total travel, 1 μm approach, 1 μm retract), which were analyzed using Nanoscope software with the implementation of a best-fit curve to a Hertzian (spherical) model (optimized such that R^2 value was greater than 0.95, or $p < 0.05$) to obtain elastic moduli of nuclear membrane of individual nuclei.

4.5.3 Simulated Microgravity Treatment

All data analysis results were displayed graphically based on the mean value with standard error bars. Differences between treatments were not assumed to follow a Gaussian distribution. Therefore, group differences were identified via either non-

parametric two-tailed Mann-Whitney U-test (Fig. 1b) or Kruskal-Wallis test followed by Tukey multiple comparison (Figures 2b, 4, 5, 6, 7 and S1). P-values of less than 0.05 were considered significant.

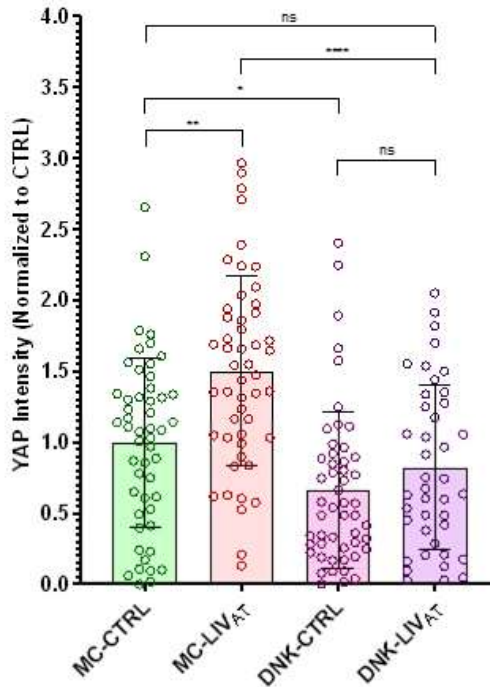


Figure S1. LINC complex disruption decreases nuclear YAP levels and reduces LIVAT-induced YAP nuclear entry sensitivity.

MSCs were cultured and treated with mCherry plasmids with (DNK) and without (MC) overexpression of a dominant negative KASH domain of Nesprin, then each group was subsequently subjected to LIV_{AT}. MATLAB image analysis of stained images revealed for MC-LIV samples 49.27% increase, for DNK-CTRL samples 33.91% decrease, and for DNK-LIV_{AT} samples 18.33% decrease of nuclear YAP levels compared to MC-CTRL levels with no significance difference between the DNK samples. n=30/grp, group comparisons were made using one-way ANOVA, ****, p<0.0001.

CHAPTER FIVE: RESEARCH CONCLUSIONS AND FUTURE

5.1 Summary of Research

The overarching experimental goals of this research were to:

- Determine if nuclear YAP levels are affected in MSCs by acute LIV
- Determine if nuclear YAP levels are affected in MSCs under SMG
- Determine if YAP nuclear entry response to acute mechanical challenge is affected in MSCs under SMG
- Determine if these effects of SMG can be counteracted by LIV

The significant results of this research include:

- A method was developed which enabled the simultaneous application of SMG and LIV treatment and also allowed for immunofluorescence staining analysis
- A form of acute LIV treatment was developed which was capable of activating YAP nuclear shuttling in MSCs
- Basal nuclear YAP levels in MSCS were found to be decreased by SMG and restored to control levels by simultaneous daily LIV treatment, showing correlation with the observed effect of these treatments on MSC proliferation
- YAP nuclear shutting response to both acute LIV treatment and LPA addition after applied SMG was found to be partially restored to control levels by daily LIV treatment

Our experimental hypothesis was confirmed:

- SMG-induced impairment of acute YAP nuclear entry in response to mechanical and soluble factors was alleviated by daily application of LIV

5.2 Current Limitations

The YAP signaling pathway is known to be connected to and affected by several other signaling pathways and is not the only pathway which affects cell proliferation. The correlation of nuclear YAP levels with cell proliferation in this research combined with YAP's known role in cell proliferation suggests that the YAP signaling pathway is a major contributing component of the mechanism which dictates the mechanoadaptive response of cells in bone and muscle tissue. However, it remains unclear which other signaling components play a role in and to what degree they are responsible for this signaling response. The primary limitation of this student was that all of the experiments were focused on the nuclear YAP content which was a useful tool for tracking YAP nuclear shuttling but could not reveal the functional effects of the SMG and LIV treatment on the MSC mechanoadaptation mechanism.

5.3 Future Directions

The significant valuable result of this research was the method which was developed to analyze YAP nuclear shuttling in response to SMG and LIV treatments. Future research attempting to understand the specific effects of these treatments on this signaling pathway should focus on the analysis of both the mechanical components and the other biochemical signaling components of the MSC mechanoadaptation mechanism. Specifically, investigation of the effects of SMG and LIV treatments on these mechanical components including cell membrane structure, cytoskeletal structure, nuclear structure,

as well as the numerous other biochemical signaling proteins followed by comparison of the these components to the YAP nuclear shuttling response using the methods developed in this study will help to comprehensively define the behavior of this mechanism.

REFERENCES

1. Vico, L., Collet, P., Guignandon, A., Lafage-Proust, M.H., Thomas, T., Rehaillia, M., Alexandre, C. Effects of long-term microgravity exposure on cancellous and cortical weight-bearing bones of cosmonauts. *Lancet* **355**, 1607-11, (2000).
2. Gadomski, B.C., McGilvray, K.C., Easley, J.T., Palmer, R.H., Santoni, B.G., Puttlitz, C.M. Partial gravity unloading inhibits bone healing responses in a large animal model. *J Biomech* **47**, 2836-42, (2014).
3. Halder, G., Dupont, S., Piccolo, S. Transduction of mechanical and cytoskeletal cues by YAP and TAZ. *Nat Rev Mol Cell Biol* **13**, 591-600, (2012).
4. Dupont, S., Morsut, L., Aragona, M., Enzo, E., Giulitti, S., Cordenonsi, M., Zanconato, F., Le Digabel, J., Forcato, M., Bicciato, S., Elvassore, N., Piccolo, S. Role of YAP/TAZ in mechanotransduction. *Nature* **474**, 179-183, (2011).
5. Benham-Pyle, B.W., Pruitt, B.L., Nelson, W.J. Mechanical strain induces E-cadherin-dependent Yap1 and β -catenin activation to drive cell cycle entry. *Science* **348**, 1024–1027, (2015).
6. Driscoll, T.P., Cosgrove, B.D., Heo, S.J., Shurden, Z.E., Mauck, R.L. Cytoskeletal to Nuclear Strain Transfer Regulates YAP Signaling in Mesenchymal *Stem Cells*. *Biophys J*, **108**, 2783–2793, (2015).
7. Touchstone, H., Bryd, R., Loiate, S., Thompson, M., Kim, S., Puranam, K., Senthilnathan, A.N., Pu, X., Beard, R., Rubin, J., Alwood, J. Oxford, J.T., Uzer, G. Recovery of stem cell proliferation by low intensity vibration under simulated microgravity requires LINC complex. *NPJ Microgravity* **5**, 11, (2019).
8. Pongkitwitoon, S., Uzer, G., Rubin, J., Judexa, S. Cytoskeletal Configuration Modulates Mechanically Induced Changes in Mesenchymal Stem Cell Osteogenesis, Morphology, and Stiffness. *Sci Rep* **6**, 34791, (2016).

9. Bonewald, L.F. (2011). The amazing osteocyte. *J. Bone Miner. Res.*, 26, 229–238.
10. Baek, M.O., Ahn, C.B., Cho, H.J., Choi, J.Y., Son, K.H., Yoon, M.S. Simulated microgravity inhibits C2C12 myogenesis via phospholipase D2-induced Akt/FOXO1 regulation. *Scientific Reports* **9**, 14910, (2019).
11. Fritton, S.P., McLeod, K.J., Rubin, C.T. Quantifying the strain history of bone: spatial uniformity and self-similarity of low-magnitude strains. *J Biomech* **33**, 317–325, (2000).
12. Albiol, L., Büttner, A., Pflanz, D., Mikolajewicz, N., Birkhold, A.I., Kramer, I., Kneissel, M., Duda, G.N., Checa S., Willie B.M. Effects of Long-Term Sclerostin Deficiency on Trabecular Bone Mass and Adaption to Limb Loading Differ in Male and Female Mice. *Calcif Tissue Int* 1–16, (2019).
13. Hwang, S.J., Lublinsky, S., Seo, Y.K., Kim, I.S., Judex, S. Extremely small-magnitude accelerations enhance bone regeneration: a preliminary study. *Clin Orthop Relat Res* **467**, 1083-1091, (2009).
14. Vogel, V., Sheetz, M. Local force and geometry sensing regulate cell functions. *Nature Rev Mol Cell Biol* **7**, 265–275, (2006).
15. Volkers L., Mechioukhi Y., Coste B. Piezo channels: from structure to function. *Pflugers Arch* **467**, 95–99. (2014).
16. Uzer, G., Thompson, W.R., Sen, B., Xie, Z., Yen, S.S., Miller, S., Bas, G., Styner, M., Rubin, C.T., Judex, S., Burrige, K., Rubin, J. Cell Mechanosensitivity to Extremely Low Magnitude Signals is Enabled by a LINCed Nucleus. *Stem Cells* **33**, 2063–2076, (2015).
17. Sen, B., Xie, Z., Case, N., Styner, M., Rubin, C.T. Rubin, J. Mechanical signal influence on mesenchymal stem cell fate is enhanced by incorporation of refractory periods into the loading regimen. *J Biomech* **44**, 593-9, (2011).
18. Greenleaf, J.E., Bulbulian, R., Bernauer, E.M., Haskell, W.L., Moore, T. Exercise-training protocols for astronauts in microgravity. *Journal of applied physiology (Bethesda, Md. : 1985)* **67**, 2191-2204, (1989).

19. Smith, S.M., Wastney, M.E., Morukov, B.V., Larina, I.M., Nyquist, L.E., Abrams, S.A., Taran, E.N., Shih, C.Y., Nillen, J.L., Davis-Street, J.E., Rice, B.L., Lane, H.W. Calcium metabolism before, during, and after a 3-mo spaceflight: kinetic and biochemical changes. *Am J Physiol* **277**, R1-10, (1999).
20. Thompson, W.R., Rubin, C.T., Rubin, J. Mechanical regulation of signaling pathways in bone. *Gene* **503**, 179-193, (2012).
21. Ozcivici, E., Luu, Y.K., Adler, B., Qin, Y.X., Rubin, J., Judex, S., Rubin, C.T. Mechanical signals as anabolic agents in bone. *Nature reviews. Rheumatology* **6**, 50-59, (2010).
22. Rando, T.A., Ambrosio, F. Regenerative Rehabilitation: Applied Biophysics Meets Stem Cell Therapeutics. *Cell Stem Cell* **22**, 306-309, (2018).
23. Chan, M.E., Uzer, G., Rubin, C. The Potential Benefits and Inherent Risks of Vibration as a Non-Drug Therapy for the Prevention and Treatment of Osteoporosis. *Current osteoporosis reports*, 1-9, (2013).
24. Judex, S., Gross, T.S., Zernicke, R.F. Strain Gradients Correlate with Sites of Exercise-Induced Bone-Forming Surfaces in the Adult Skeleton. *Journal of Bone and Mineral Research* **12**, 1737-1745, (1997).
25. Rubin, C.T., Lanyon, L.E. Dynamic strain similarity in vertebrates; an alternative to allometric limb bone scaling. *Journal of Theoretical Biology* **107**, 321-327, (1984).
26. Price, C., Zhou, X.Z., Li, W., Wang, L.Y. Real-Time Measurement of Solute Transport Within the Lacunar-Canalicular System of Mechanically Loaded Bone: Direct Evidence for Load-Induced Fluid Flow. *Journal of Bone and Mineral Research* **26**, 277-285, (2011).
27. Gurkan, U.A., Akkus, O. The Mechanical Environment of Bone Marrow: A Review. *Annals of biomedical engineering* **36**, 1978-1991, (2008).
28. Vainionpaa, A., Korpelainen, R., Vihriala, E., Rinta-Paavola, A., Leppaluoto, J., Jamsa, T. Intensity of exercise is associated with bone density change in premenopausal women. *Osteoporosis international : a journal established as result of*

- cooperation between the European Foundation for Osteoporosis and the National Osteoporosis Foundation of the USA* **17**, 455-463, (2006).
29. Dickerson, D.A., Sander, E.A., Nauman, E.A., Modeling the mechanical consequences of vibratory loading in the vertebral body: microscale effects. *Biomechanics and Modeling in Mechanobiology* **7**, 191-202, (2008).
 30. Coughlin, T.R., Niebur, G.L. Fluid shear stress in trabecular bone marrow due to low-magnitude high-frequency vibration. *Journal of biomechanics* **45**, 2222-2229, (2012).
 31. Riddle, R.C., Donahue, H.J. From Streaming Potentials to Shear Stress: 25 Years of Bone Cell Mechanotransduction. *Journal of Orthopaedic Research* **27**, 143-149, (2009).
 32. Pagnotti, G.M., Styner, M., Uzer, G., Patel, V.S., Wright, L.E., Ness, K.K., Guise, T.A., Rubin, J., Rubin, C.T. Combating osteoporosis and obesity with exercise: leveraging cell mechanosensitivity. *Nature Reviews Endocrinology*, (2019).
 33. Uzer, G., Pongkitwitoon, S., Ete Chan, M., Judex, S. Vibration induced osteogenic commitment of mesenchymal stem cells is enhanced by cytoskeletal remodeling but not fluid shear. *Journal of biomechanics* **46**, 2296-2302, (2013).
 34. Pan, J.X., Xiong, L., Zhao, K., Zeng, P., Wang, B., Tang, F.L., Sun, D., Guo, H.H., Yang, X., Cui, S., Xia, W.F., Mei, L., Xiong, W.C. YAP promotes osteogenesis and suppresses adipogenic differentiation by regulating beta-catenin signaling. *Bone research* **6**, 18, (2018).
 35. Kegelman, C.D., Mason, D.E., Dawahare, J.H., Horan, D.J., Vigil, G.D., Howard, S.S., Robling, A.G., Bellido, T.M., Boerckel, J.D. Skeletal cell YAP and TAZ combinatorially promote bone development. *FASEB journal : official publication of the Federation of American Societies for Experimental Biology* **32**, 2706-2721, (2018).
 36. Zhao, B., Ye, X., Yu, J., Li, L., Li, W., Li, S., Yu, J., Lin, J.D., Wang, C.Y., Chinnaiyan, A.M., Lai, Z.C., Guan, K.L. TEAD mediates YAP-dependent gene induction and growth control. *Genes & development* **22**, 1962-1971, (2008).

37. Cai, H., Xu, Y. The role of LPA and YAP signaling in long-term migration of human ovarian cancer cells. *Cell Communication and Signaling* **11**, 31, (2013).
38. Ho, L.T.Y., Skiba, N., Ullmer, C., Rao, P.V. Lysophosphatidic Acid Induces ECM Production via Activation of the Mechanosensitive YAP/TAZ Transcriptional Pathway in Trabecular Meshwork Cells. *Investigative Ophthalmology & Visual Science* **59**, 1969-1984, (2018).
39. Janmaleki, M., Pachenari, M., Seyedpour, S.M., Shahghadami, R., Sanati-Nezhad, A. Impact of Simulated Microgravity on Cytoskeleton and Viscoelastic Properties of Endothelial Cell. *Sci Rep* **6**, 32418, (2016).
40. Pardo, S.J., Patel, M.J., Sykes, M.C., Platt, M.O., Boyd, N.L., Sorescu, G.P., Xu, M., van Loon, J.J., Wang, M.D., Jo, H. Simulated microgravity using the Random Positioning Machine inhibits differentiation and alters gene expression profiles of 2T3 preosteoblasts. *Am J Physiol Cell Physiol* **288**, (2005).
41. Qian, A.R., Li, D., Han, J., Gao, X., Di, S.M., Zhang, W., Hu, L.F., Peng, S. Fractal Dimension as a Measure of Altered Actin Cytoskeleton in MC3T3-E1 Cells Under Simulated Microgravity Using 3-D/2-D Clinostats. *Biomedical Engineering, IEEE Transactions on* **59**, 1374-1380, (2012).
42. Corydon, T.J., Mann, V., Slumstrup, L., Kopp, S., Sahana, J., Askou, A.L., Magnusson, N.E., Echevoyen, D., Bek, T., Sundaresan, A., Riwaldt, S., Bauer, J., Infanger, M., Grimm, D. Reduced Expression of Cytoskeletal and Extracellular Matrix Genes in Human Adult Retinal Pigment Epithelium Cells Exposed to Simulated Microgravity. *Cellular physiology and biochemistry : international journal of experimental cellular physiology, biochemistry, and pharmacology* **40**, 1-17, (2016).
43. Shi, F., Wang, Y.C., Hu, Z.B., Xu, H.Y., Sun, J., Gao, Y., Li, X.T., Yang, C.B., Xie, C., Li, C.F., Zhang, S., Zhao, J.D., Cao, X.S., Sun, X.Q. Simulated Microgravity Promotes Angiogenesis through RhoA-Dependent Rearrangement of the Actin Cytoskeleton. *Cellular physiology and biochemistry : international journal of*

- experimental cellular physiology, biochemistry, and pharmacology* **41**, 227-238, (2017).
44. Shiu, J.Y., Aires, L., Lin, Z., Vogel, V. Nanopillar force measurements reveal actin-cap-mediated YAP mechanotransduction. *Nat Cell Biol* **20**, 262-271, (2018).
 45. Saeed, M., Weihs, D. Finite element analysis reveals an important role for cell morphology in response to mechanical compression. *Biomechanics and Modeling in Mechanobiology*, (2019).
 46. Riddick, N., Ohtani, K., Surks, H.K., Targeting by myosin phosphatase-RhoA interacting protein mediates RhoA/ROCK regulation of myosin phosphatase. *Journal of Cellular Biochemistry* **103**, 1158-1170, (2008).
 47. Czapiewski, R., Robson, M.I., Schirmer, E.C., Anchoring a Leviathan: How the Nuclear Membrane Tethers the Genome. *Frontiers in genetics* **7**, 82, (2016).
 48. De Magistris, P., Antonin, W. The Dynamic Nature of the Nuclear Envelope. *Current biology : CB* **28**, R487-r497, (2018).